Antiferromagnetic, metal-insulator, and superconducting phase transitions in underdoped cuprates: Slave-fermion t-J model in the hopping expansion

Akihiro Shimizu*, Koji Aoki*, Kazuhiko Sakakibara⋆, Ikuo Ichinose*, and Tetsuo Matsui†
*Department of Applied Physics, Graduate School of Engineering,
Nagoya Institute of Technology, Nagoya, 466-8555 Japan
⋆Department of Physics, Nara National College of Technology, Yamatokohriyama, 639-1080 Japan and
†Department of Physics, Kinki University, Higashi-Osaka, 577-8502 Japan

(Dated: July 27, 2010)

In the present paper, we study a system of doped antiferromagnet in three dimensions at finite temperatures by using the t-J model, a canonical model of strongly-correlated electrons. We employ the slave-fermion representation of electrons in which an electron is described as a composite of a charged spinless holon and a chargeless spinon. We introduce two kinds of U(1) gauge fields on links as auxiliary fields, one describing resonating valence bonds of antiferromagnetic nearest-neighbor spin pairs and the other for nearest-neighbor hopping amplitudes of holons and spinons in the ferromagnetic channel. In order to perform numerical study of the system, we integrate out the fermionic holon field by using the hopping expansion in powers of the hopping amplitude, which is legitimate for the region in and near the insulating phase. The resultant effective model is described in terms of bosonic spinons and the two U(1) gauge fields, and a collective field for hole pairs. We study this model by means of Monte-Carlo simulations, calculating the specific heat, spin correlation functions, and instanton densities. We obtain a phase diagram in the hole concentration-temperature plane, which is in good agreement with that observed recently for clean and homogeneous underdoped samples.

PACS numbers: 74.72.-h, 11.15.Ha, 74.25.Dw

I. INTRODUCTION

Since the discovery of high-temperature superconductors of cuprates, it has passed more than two decades[1]. Besides their high critical temperatures (T) of superconducting (SC) phase transition, these cuprates have several interesting properties like anomalous properties in the metallic state, existence of Fermi arcs, etc[2]. To explain these properties, various theoretical approaches have been proposed[3]. Although ample knowledge have been accumulated, we still do not have a theory that has been proved and accepted as a "right" one.

The t-J model[4] is regarded as one of the canonical models for high-T_c cuprates. The model excludes doubly-occupied electron states at each site reflecting the strong correlations (Coulomb repulsion) among electrons. This condition makes it hard to get convincing and solid understanding of the model such as its phase structure.

The slave-particle approach[5] using the slave-fermion (SF) or the slave-boson representation has been proposed in order to treat this local constraint on the physical states faithfully. In the SF representation, each electron is described as a composite of a charged spinless fermionic particle called holon and a neutral bosonic particle with spin called spinon. The SF approach is known to be superior[6] (giving a lower ground-state energy in the mean-field theory) than its statistics-reversed assignment, the slave-boson representation, in the region with small hole concentrations δ (δ is just the density of holons per site).

We have studied the SF t-J model in path-integral formalism[7]. Let us summarize the results of Ref.[7]. The local constraint is exactly respected by using the CP^1 (complex projective) variables (we write it $z_{x\sigma}$ in Sect.II) for spinons. The fermionic holons (ψ_x) are described by Grassmann numbers. In path-integral expression of the partition function, fluctuations of variables along the imaginary time give rise to certain imaginary term in the action. By assuming the short-range antiferromagnetic (AF) order between the nearest-neighbor (NN) spin pair, we integrated over a half of the spinon variables, those sitting at the odd sites, assuming a short-range (SR) AF order to obtain an effective model. At the half filling ($\delta = 0$) the effective model reduces to the Heisenberg spin model. It favors the so-called resonating valence bonds (RVB), the NN spin singlet pairs with AF coupling. As holons are doped, the AF order are gradually destroyed because hopping of holons is associated by hopping of spinons without spin flips, which breaks some RVB's.

Also there arises an attractive force between NN holon pair reflecting the energy released by breaking RVB's. In fact, the NN holon pair breaks only 7(11) RVB's while a holon pair separated at longer distance breaks 8(12) RVB's in two(three)-dimensional lattice. In Ref.[7], we have introduced a hole-pair field, the condensation of which implies the SC state, and derived its Ginzburg-Landau (GL) model in the hopping expansion. At the mean-field level, this GL favors the so-called flux phase corresponding to $(s + id)$-wave symmetry.

The slave-particle approach intrinsically possesses U(1) gauge symmetry, since the electron operator is invariant under the local and simultaneous rotation of phases of holon and spinon fields. The possible charge-spin separation phenomena[8] has a natural and poten-

tially simple explanation such that the U(1) gauge dynamics in cuprates is realized in the deconfinement phase. In fact, in the deconfinement phase, holons and spinons may appear as unbound quasiparticles moving independently due to the weak gauge force among them.

The slave-particle approach has yet another advantage. The mean field theory based on the slave-particle representation is basically capable to describe various expected phases including the SC phase[9]. However, the criticism to this result may be common to every mean field theory, i.e., the faithful evaluation of effects of fluctuations around mean fields are missing. It is rather hard to evaluate such effects analytically in nonperturbative manner because the model has local gauge symmetry as mentioned and associated zero modes may give rise to strong effects in the infrared region.

One may think that numerical studies may be one viable approach as the successful example of lattice gauge theory in high-energy physics demonstrates. However, straightforward numerical studies such as Monte-Carlo (MC) simulations of the SF t-J model in path-integral representation are still not feasible because of the notorious sign problem in the fermionic determinant generated upon integrating over holon variables.

In the present paper, we shall revisit the t-J model on a three-dimensional (3D) lattice in the SF path-integral representation with the purpose to study its nonperturbative aspects by numerical methods. In order to avoid the difficulty associated with fermionic determinant mentioned above, we derive an effective model by employing the hopping expansion to evaluate integrals over fermionic holons. It is an expansion in powers of the hopping amplitude of holons. An effective expansion parameter is $t \times \delta$, so the expansion is useful and legitimate at sufficiently low dopings δ. In the region of applicability of the hopping expansion, the wild behavior of fermionic determinant is suppressed in a natural way. We respect the structure of interaction terms generated by the hopping expansion, but consider their coefficients as independent parameters in a flexible manner. This is partly because these coefficients acquire renormalization via higher-order terms in the expansion.

As mentioned, the action in path-integral representation involves the imaginary part reflecting the imaginary-time dependence of the variables. This brings some complications in numerical approach. In Ref.[7] we have seen that the integration over odd-site spinon variables makes the spinon part of the resultant action real. In this paper, we avoid this imaginary part in another manner by simply considering the region of finite T's; at sufficiently high T such that the dependence of variables on the imaginary time may be neglected. We expect that each phase obtained at finite T's survives down to sufficiently low T's including $T = 0$, so the obtained phase diagram at finite T's is useful not only for itself but also for low T's down to $T = 0$.

In the practical numerical study, knowledge and techniques developed in the study of lattice gauge theory of high-energy physics are helpful. By making MC simulations of the effective model, we obtain a phase diagram in the δ-T plane, which contains AF phase, SC phase, and metal-insulator (MI) transition. The overall phase structure is similar to that observed in experiments for lightly-doped materials[10].

The present paper is organized as follows. In Sect.II, we explain and set up the model in detail. The holon variables are analytically integrated out by means of the hopping expansion to obtain the effective model at small δ's and finite T's. The model includes several variables; (i) the spinon field $z_{x\sigma}$, (ii) the auxiliary field for spin-singlet (RVB) amplitude of NN spinon pair (we call it $U_{x\mu}$ in Sect.II), (iii) the auxiliary field for amplitude of holon and spinon hoppings in the ferromagnetic (FM) channel ($V_{x\mu}$), which works as an order parameter of the MI transition, and (v) the hole-pair field ($M_{x\mu}$) for superconductivity. We introduce the hole-pair field and include the associated GL terms to the effective action, respecting the NN attractive force between holons as discussed in Ref.[7].

In Sect.III, we first study the case without the superconducting channel (by neglecting the GL energy of hole-pair field). We present the results of MC simulations for the corresponding model, which we call UV model. We calculated spin correlation function to study the AF transition, and instanton densities of U-field and V-field to study the decay of AF order and the MI transition. We locate the AF and MI phase transition lines.

In Sect.IV, we study the full model including the SC channel and discuss SC phase transition together with AF and MI ones. We modify the coefficients of GL terms of hole pairs from the leading-order values of hopping expansion of Ref.[7] so as to describe the d-wave SC observed in experiments instead of $s + id$ one. This is because the SC transition is expected (and actually verified later on) to occur in the metallic phase and the higher-order terms of the hopping expansion should be included. Our standpoint is that we regard the hole-pair part of the effective model in a flexible manner, i.e., its structure is suggested by hopping expansion but its coefficients are relaxed to study the region beyond the validity of the leading order of the hopping expansion. We find that the SC state occurs always in the metallic phase, whereas the AF long-range order (LRO) can coexist with the SC. There appear two phase transitions related with the SC. One is a primordial SC transition that stabilizes the amplitude of hole pairs and gives rise to a pseudo-gap in holon excitation energy, while the other is a genuine SC transition reflecting a phase coherence of hole pairs associated with the Higgs mechanism.

In Sect.V we present discussions and conclusions. We discuss that the present model offers us an interesting possibility of new description of a SC state in the framework of gauge theory with *local interactions*.

In Appendix A we give some details of the hopping expansion of path-integral over holons.

II. THE t-J MODEL IN THE SLAVE-FERMION REPRESENTATION AND HOLON HOPPING EXPANSION

A. Path integral expression

We start with the standard t-J model on a 3D cubic lattice[11], whose Hamiltonian is given in terms of electron operator $C_{x\sigma}$ at site x $(= x_1, x_2, x_3)$ and spin σ $[= 1(\uparrow), 2(\downarrow)]$ as follows;

$$H = -t\sum_{x,\mu,\sigma}\left(\tilde{C}^\dagger_{x+\mu,\sigma}\tilde{C}_{x\sigma} + \text{H.c.}\right) + J\sum_{x,\mu}\Big[\vec{S}_{x+\mu}\cdot\vec{S}_x - \frac{1}{4}n_x n_{x+\mu}\Big], \tag{2.1}$$

where

$$\tilde{C}_{x\sigma} \equiv (1 - C^\dagger_{x\bar{\sigma}}C_{x\bar{\sigma}})\ C_{x\sigma},$$
$$\vec{S}_x \equiv \frac{1}{2}\sum_{\sigma,\sigma'} C^\dagger_{x\sigma}\vec{\sigma}_{\sigma\sigma'}C_{x\sigma'},\quad (\vec{\sigma}: \text{Pauli matrices}),$$
$$n_x \equiv \sum_\sigma C^\dagger_{x\sigma}C_{x\sigma}. \tag{2.2}$$

$\mu(= 1, 2, 3)$ is the 3D direction index and also denotes the unit vector. $\bar{\sigma}$ $(\bar{1} \equiv 2, \bar{2} \equiv 1)$ denotes the opposite spin. The doubly occupied states $(C^\dagger_{x\uparrow}C^\dagger_{x\downarrow}|0\rangle)$ are excluded from the physical states due to the strong on-site Coulomb repulsion. The operator $\tilde{C}_{x\sigma}$ respects this point.

We adopt the *slave-fermion representation* of the electron operator $C_{x\sigma}$ as a composite form,

$$C_{x\sigma} = \psi^\dagger_x a_{x\sigma}, \tag{2.3}$$

where ψ_x represents annihilation operator of the fermionic holon carrying the charge e and no spin and $a_{x\sigma}$ represents annihilation operator of the bosonic spinon carrying $s = 1/2$ spin and no charge. Physical states $|\text{Phys}\rangle$ satisfy the following constraint,

$$\Big(\sum_\sigma a^\dagger_{x\sigma}a_{x\sigma} + \psi^\dagger_x\psi_x\Big)|\text{phys}\rangle = |\text{phys}\rangle. \tag{2.4}$$

In the salve-fermion representation, the Hamiltonian (2.1) is given as

$$H = -t\sum_{x,\mu}\Big(\psi^\dagger_x a^\dagger_{x+\mu}a_x\psi_{x+\mu} + \psi^\dagger_{x+\mu}a^\dagger_x a_{x+\mu}\psi_x\Big) + \frac{J}{4}\sum_{x,\mu}\Big[(a^\dagger\vec{\sigma}a)_{x+\mu}\cdot(a^\dagger\vec{\sigma}a)_x - (a^\dagger a)_{x+\mu}(a^\dagger a)_x\Big],$$
$$(a^\dagger a)_x \equiv \sum_\sigma a^\dagger_{x\sigma}a_{x\sigma},\ (a^\dagger\vec{\sigma}a)_x \equiv \sum_{\sigma,\sigma'} a^\dagger_{x\sigma}\vec{\sigma}_{\sigma\sigma'}a_{x\sigma'}. \tag{2.5}$$

We employ the path-integral expression for the partition function of the t-J model,

$$Z = \text{Tr}\exp(-\beta H),\quad \beta \equiv \frac{1}{k_\text{B}T}, \tag{2.6}$$

at finite T in the slave-fermion representation. This is done by introducing a complex number $a_{x\sigma}(\tau)$ and a Grassmann number $\psi_x(\tau)$ at each site x and the imaginary time $\tau \in [0, \beta]$. The constraint (2.4) is solved[7] by introducing CP^1 spinon variable $z_{x\sigma}(\tau)$, i.e., two complex numbers z_{x1}, z_{x2} for each site x satisfying

$$\sum_\sigma \bar{z}_{x\sigma}z_{x\sigma} = 1, \tag{2.7}$$

and writing

$$a_{x\sigma} = (1 - \bar{\psi}_x\psi_x)^{1/2}z_{x\sigma}. \tag{2.8}$$

It is easily verified that the constraint (2.4) is satisfied by Eqs.(2.8) and (2.7). Then, the partition function in the path-integral representation is given by an integral over the CP^1 variables $z_{x\sigma}(\tau)$ and Grassmann numbers $\psi_x(\tau)$.

We shall consider the system at finite and relatively high T's, such that *the $\tau-$dependence of the variables $z_{x\sigma}, \psi_x$ are negligible* (i.e., only their zero modes survive). Then the kinetic terms of $z_{x\sigma}, \psi_x$ like $\bar{z}_x\partial z_x/\partial\tau, \bar{\psi}_x\partial\psi_x/\partial\tau$ disappear, and the T-dependence may appear only as an overall factor β, which may be absorbed into the coefficients of the action and one may still deal with the 3D model instead of the four-dimensional model. Study of finite-T properties of the systems gives us an important insight into the low-T phase structure, for we can expect that ordered phase at finite-T generally survives at $T = 0$.

In this way, the partition function Z of the 3D model at finite T's is given by the path integral[7],

$$Z = \int [dz][d\psi][dU]\exp A, \tag{2.9}$$
$$[dz] = \prod_x dz_x,\ [d\psi] = \prod_x d\psi_x d\bar{\psi}_x,\ [dU] = \prod_{x,\mu} dU_{x\mu},$$

with the following action A on the 3D lattice[12, 13],

$$A = A_\text{AF} + A_\text{hop} + A_\text{SC},$$
$$A_\text{AF} = \frac{c_1}{2}\sum_{x,\mu}\Big(z^\star_{x+\mu}U_{x\mu}z_x + \text{c.c.}\Big),$$
$$A_\text{hop} = \frac{c_3}{2}\sum_{x,\mu}\left(\bar{z}_{x+\mu}z_x\bar{\psi}_x\psi_{x+\mu} + \text{c.c.}\right) - m\sum_x \rho_x,$$
$$A_\text{SC} = \frac{J\beta}{2}\sum_{x,\mu}\rho_{x+\mu}\rho_x|z^\star_{x+\mu}z_x|^2, \tag{2.10}$$

where

$$U_{x\mu} \equiv \exp(i\theta_{x\mu})\ \in U(1),$$
$$\rho_x \equiv \bar{\psi}_x\psi_x,$$
$$\bar{z}_{x+\mu}z_x \equiv \bar{z}_{x+\mu,1}z_{x1} + \bar{z}_{x+\mu,2}z_{x2}$$
$$z^\star_{x1} \equiv z_{x2},\ z^\star_{x2} \equiv -z_{x1},$$
$$z^\star_{x+\mu}z_x = z_{x+\mu,2}z_{x1} - z_{x+\mu,2}z_{x1}. \tag{2.11}$$

The first term A_AF in the action A describes the AF coupling between NN spinons. We have introduced the

U(1) gauge field $U_{x\mu}$ on the link $(x, x+\mu)$ as an auxiliary field to make the action in a simpler form and the U(1) gauge invariance (explained below) manifest. The second term $A_{\rm hop}$ describes simultaneous NN hopping of a holon and a spinon keeping its spin orientation (i.e., in the FM channel). The third term $A_{\rm SC}$ describes attractive force between hole pairs, which we shall discuss in Sect.IID in detail. There are remaining terms[14], which are irrelevant to discuss the global phase structure.

The integration measure of $z_{x\sigma}$ and $U_{x\mu}$ are

$$\int dz_x = \prod_\sigma \int_{-\infty}^{\infty} d\,{\rm Re} z_{x\sigma} \int_{-\infty}^{\infty} d\,{\rm Im} z_{x\sigma} \cdot \delta(\sum_\sigma \bar{z}_{x\sigma} z_{x\sigma} - 1),$$
$$\int dU_{x\mu} = \int_{-\pi}^{\pi} \frac{d\theta_{x\mu}}{2\pi}. \tag{2.12}$$

Grassmann variables ψ_x anti-commute each other,

$$[\psi_x, \psi_{x'}]_+ = [\psi_x, \bar{\psi}_{x'}]_+ = [\bar{\psi}_x, \bar{\psi}_{x'}]_+ = 0. \tag{2.13}$$

The formulae of Grassmann integration[15] are

$$\int d\psi_x d\bar{\psi}_x [1, \psi_x, \bar{\psi}_x, \bar{\psi}_x \psi_x] = [0, 0, 0, 1]. \tag{2.14}$$

The term $m \sum_x \bar{\psi}_x \psi_x$ adjust the hole density to δ as

$$\langle \bar{\psi}_x \psi_x \rangle = \delta. \tag{2.15}$$

Therefore the parameter m works as (the minus of) the chemical potential.

The action A is invariant under a local (x-dependent) U(1) gauge transformation with a gauge function λ_x[16],

$$\begin{aligned} z_{x\sigma} &\to e^{i\lambda_x} z_{x\sigma}, \\ U_{x\mu} &\to e^{-i\lambda_{x+\mu}} U_{x\mu} e^{-i\lambda_x}, \\ \psi_x &\to e^{i\lambda_x} \psi_x. \end{aligned} \tag{2.16}$$

B. AF and Ferromagnetic spinon amplitudes

The gauge field $U_{x\mu}$ is related to the spinon field z_x as

$$\langle U_{x\mu} \rangle \sim \overline{\left\langle \frac{z^\star_{x+\mu} z_x}{|z^\star_{x+\mu} z_x|} \right\rangle}, \tag{2.17}$$

which is obtained by maximizing the action $A_{\rm AF}$. Therefore $U_{x\mu}$ describes the (c.c. of) phase factor of AF NN spin-pair amplitude $z^\star_{x+\mu} z_x$ of Eq.(2.11). In fact, one can integrate out $U_{x\mu}$ in Eq.(2.9) and obtain

$$\begin{aligned} \int [dU] \exp(A_{\rm AF}) &= \exp(\tilde{A}_{\rm CP^1}), \\ \tilde{A}_{\rm CP^1} &= \sum_{x\mu} \log I_0(c_1 |z^\star_{x+\mu} z_x|), \end{aligned} \tag{2.18}$$

where I_0 is the modified Bessel function. The effective term $\tilde{A}_{\rm CP^1}$ should be compared with the original expression $A_{\rm CP^1}$ of the CP^1 model,

$$\begin{aligned} Z_{\rm CP^1} &= \int [dz] \exp(A_{\rm CP^1}), \\ A_{\rm CP^1} &= \frac{\beta J}{2} \sum_{x,\mu} \left| z^\star_{x+\mu} z_x \right|^2. \end{aligned} \tag{2.19}$$

This CP^1 model describes the t-J model without holes ($c_3 = 0$, $A_{\rm SC} = 0$), i.e., AF Heisenberg spin model at finite T. Note that the amplitude $z^\star_{x+\mu} z_x$ between NN spinon pair reads explicitly as

$$z^\star_{x+\mu} z_x = z_{x+\mu,2} z_{x1} - z_{x+\mu,1} z_{x2}. \tag{2.20}$$

This expresses the amplitude of spin-singlet AF combination of NN spinons, which is called the RVB. Both models with $A_{\rm CP^1}$ and $\tilde{A}_{\rm CP^1}$ have similar behavior and it is verified that they give rise to second-order transitions at certain c_1 and J[17]. The parameters c_1 in the action (2.10) are related to the original ones as[17]

$$c_1 \sim \begin{cases} J\beta & \text{for } c_1 \gg 1, \\ (2J\beta)^{1/2} & \text{for } c_1 \ll 1, \end{cases} \tag{2.21}$$

For the coupling c_3, the relation is straightforward,

$$c_3 \sim t\beta. \tag{2.22}$$

Let us see the meaning of CP^1 term $A_{\rm AF}$ (the AF spin coupling) and the hopping term $A_{\rm hop}$ (the t-term) further. For this purpose, it is convenient to introduce an O(3) spin vector field $\vec{\ell}_x$ made of spinon z_x,

$$\vec{\ell}_x \equiv \bar{z}_x \vec{\sigma} z_x = \sum_{\sigma,\sigma'} \bar{z}_{x\sigma} \vec{\sigma}_{\sigma\sigma'} z_{x\sigma'}, \quad \vec{\ell}_x \cdot \vec{\ell}_x = 1. \tag{2.23}$$

The NN spin correlation $\vec{\ell}_{x+\mu} \cdot \vec{\ell}_x$ is expressed by the CP^1 amplitudes (such as $\bar{z}_{x+\mu} z_x$) as

$$\begin{aligned} \vec{\ell}_{x+\mu} \cdot \vec{\ell}_x &= 2|\bar{z}_{x+\mu} z_x|^2 - 1 \\ &= -2|z^\star_{x+\mu} z_x|^2 + 1, \end{aligned} \tag{2.24}$$

where we have used the identity,

$$|\bar{z}_{x+\mu} z_x|^2 + |z^\star_{x+\mu} z_x|^2 = 1. \tag{2.25}$$

So if the spinon hopping amplitude $\bar{z}_{x+\mu} z_x$ which appears in $A_{\rm hop}$ has an absolute value near its maximum, $|\bar{z}_{x+\mu} z_x| \sim 1$, then the NN spins are mostly FM $\vec{\ell}_{x+\mu} \cdot \vec{\ell}_x \sim 1$. On the other hand, if the spinon RVB amplitude $z^\star_{x+\mu} z_x$ takes values with $|z^\star_{x+\mu} z_x| \sim 1$, then the NN spins are mostly AF, $\vec{\ell}_{x+\mu} \cdot \vec{\ell}_x \sim -1$. These two amplitudes satisfy the sum rule (2.25). The AF phase and FM phase are characterized by the LRO in the spin correlation function $\langle \vec{\ell}_x \cdot \vec{\ell}_y \rangle$, and they can coexist with each other as we see in the following sections.

C. Holon hopping expansion and auxiliary field $V_{x\mu}$

In Eq.(2.9), one can integrate out the fermionic holon field ψ_x by assuming small holon density δ of Eq.(2.15). In this region, the hopping expansion of ψ_x is applicable as it is an expansion in powers of δ. Some details of

the integration of ψ_x are given in Appendix A. After integration over ψ_x we obtain

$$\int [d\psi] \exp(A_{\rm hop}) = \exp(\tilde{A}_{\rm hop}),$$
$$\tilde{A}_{\rm hop} = \delta\Big(\frac{c_3}{2}\Big)^2 \sum_{x,\mu} \big|\bar{z}_{x+\mu} z_x\big|^2 + \delta\Big(\frac{c_3}{2}\Big)^4 \sum_{x,\mu<\nu} \prod_{\rm plaq.} (\bar{z}_{x+\mu} z_x) + \cdots . \quad (2.26)$$

The second term of $\tilde{A}_{\rm hop}$ denote the product of $\bar{z}_{x+\mu} z_x$ on the link $(x, x+\mu)$ [$\bar{z}_x z_{x+\mu}$ on the link $(x+\mu, x)$] around the plaquette $(x, x+\mu, x+\mu+\nu, x+\nu)$ and the ellipsis denotes non-local higher-order terms. Both the first and the second terms favor FM couplings of NN spin pairs.

Then we introduce a vector field $W_{x\mu}$ as an auxiliary field corresponding to $\bar{z}_x z_{x+\mu}$,

$$\langle W_{x\mu} \rangle \sim \langle \bar{z}_x z_{x+\mu} \rangle, \quad (2.27)$$

by using Gaussian integration (Hubbard-Stratonovich transformation) as follows,

$$\exp(\tilde{A}_{\rm hop}) = \int [dW] \exp(A_W),$$
$$A_W = \delta\Big(\frac{c_3}{2}\Big)^2 \Big(- \sum_{\rm x,\mu} |W_{x\mu}|^2 + \sum_{x,\mu} (\bar{z}_{x+\mu} z_x W_{x\mu} + {\rm c.c.}) \Big) + \delta\Big(\frac{c_3}{2}\Big)^4 \sum_{x,\mu<\nu} \prod_{\rm plaq.} W_{x\mu} + \cdots . \quad (2.28)$$

Estimation of the magnitude of $W_{x\mu}$ is straightforward for $T/J \lesssim 1$ as

$$\int [dz] e^{-\frac{J}{2}\beta |\bar{z}_{x+\mu} z_x|^2} |\bar{z}_{x+\mu} z_x|^2 \sim \frac{1}{J\beta}. \quad (2.29)$$

Then we set

$$W_{x\mu} = W V_{x\mu}, \quad W \simeq \frac{1}{\sqrt{J\beta}},$$
$$V_{x\mu} = \exp(i\phi_{x\mu}) \ \in {\rm U(1)}, \quad (2.30)$$

by ignoring the fluctuation of radial component of $W_{x\mu}$ and focusing on its phase, $dW_{x\mu} \to dV_{x\mu} \equiv d\phi_{x\mu}/(2\pi)$. So the correspondence (2.27) becomes

$$\langle V_{x\mu} \rangle \sim \Big\langle \frac{\bar{z}_x z_{x+\mu}}{|\bar{z}_x z_{x+\mu}|} \Big\rangle. \quad (2.31)$$

This simplification is based on the observation that the most relevant degrees of freedom in gauge theories are the phases of gauge fields on the links rather than the amplitude W because the latter has only massive excitations. The phase factor $V_{x\mu}$ is a new U(1) gauge field that transforms under the gauge transformation (2.16) as

$$V_{x\mu} \to e^{i\lambda_{x+\mu}} V_{x\mu} e^{-i\lambda_x}. \quad (2.32)$$

Physical meaning of $V_{x\mu}$ is obvious from the discussion given in Sect.IIB. It measures the phase part of SR FM spinon channel, the deviation from the AF order. Its coherent "condensation" induces coherent hopping of holons ψ_x in the FM spinon channel as the term $A_{\rm hop}$ shows, and therefore a MI transition into a metallic phase. More detailed discussion will be given in the following sections.

The $A_{\rm hop}$ term is then rewritten effectively as follows,

$$\exp(\tilde{A}_{\rm hop}) = \int [dV] \exp(A_V),$$
$$A_V = \frac{c_4}{2} \sum_{x,\mu} (V_{x\mu} \bar{z}_{x+\mu} z_x + {\rm c.c.}) + \frac{c_5}{2} \sum_{x,\mu<\nu} \big(\bar{V}_{x\nu} \bar{V}_{x+\nu,\mu} V_{x+\mu,\nu} V_{x\mu} + {\rm c.c.}\big),$$
$$\int [dV] = \prod_{x,\mu} \int_{-\pi}^{\pi} \frac{d\phi_{x\mu}}{2\pi}. \quad (2.33)$$

We have neglected the higher-order terms in Eq.(2.26) as they have smaller coefficients for $T/J < 1$ with numerical damping factors. However, effects of these non-local terms can be expected qualitatively. As they have all positive coefficients, all of them favor the order of the field $V_{x\mu}$ and so the metallic phase. From this point of view, the critical hole concentration δ_c of the MI transition obtained by the numerical study in Sect.IV might give an overestimation for the true value.

The parameters c_4 and c_5 in A_V are related to the original ones as

$$c_4 \sim \frac{\delta c_3^2}{J\beta} \sim \frac{\delta t^2 \beta}{J},$$
$$c_5 \sim \frac{\delta c_3^4}{(J\beta)^2} \sim \frac{\delta t^4 \beta^2}{J^2}. \quad (2.34)$$

In the following investigation of the phase diagram of the system, however, we treat c_4 and c_5 in more flexible manner as free parameters that are proportional to δ and are increasing functions of $\beta = 1/T$. As most of phase transitions in the present model appear in the region $c_1 \gg 1$, we identify T and δ from Eqs.(2.21, 2.34) as

$$T \simeq \frac{J}{c_1}, \quad \delta \simeq \frac{J^2}{t^2} \frac{c_4}{c_1}. \quad (2.35)$$

At this stage, the original partition function Z without A_M is expressed as

$$Z \to Z_{UV} \equiv \int [dz][dU][dV] \exp(A_{UV}),$$
$$A_{UV} = A_{\rm AF}(z_x, U_{x\mu}) + A_V(z_x, V_{x\mu}). \quad (2.36)$$

This "UV" model describes the competition between the AF-RVB spin-pair amplitude $U_{x\mu}$ and the FM spin-hopping amplitude $V_{x\mu}$, the latter is generated by integration over holon hopping.

D. Hole-pair field $M_{x\mu}$ and the full model $A_{\rm full}$

As shown in the previous section, in the effective action (2.10), there exists the term $A_{\rm SC}$ that describes an attractive force between NN holes doped in AF magnets, or more precisely, in a SR AF background. This attractive force comes from the J-terms in the Hamiltonian (2.5). Actually, the two holes with a mutual distance more than one lattice spacing break twelve AF bonds of spins, while a pair of holes at NN sites break just eleven AF bonds. Thus the NN hole pair is favored energetically. To see it explicitly, we rewrite $A_{\rm SC}$ in Eq.(2.10) as follows,

$$A_{\rm SC} = \frac{J\beta}{2}\sum_{x,\mu}\Big|\bar\psi_{x+\mu}\big(z^\star_{x+\mu}z_x\big)\bar\psi_x\Big|^2. \tag{2.37}$$

Note that the holon-pair variable $\bar\psi_{x+\mu}\bar\psi_x$ is accompanied with the RVB spinon-pair amplitude $z^\star_{x+\mu}z_x$. This combination is nothing but $C_{x+\mu,2}C_{x1} - C_{x+\mu,1}C_{x2}$ in terms of electron operators. We expect that this attractive force induces hole-pair condensation under certain conditions, and as a result, a SC state is generated. The main problem to be addressed here is whether the above attractive force is strong enough to generate a SC state in the region *without* AF LRO.

In order to investigate a possible SC phase transition, we introduce a hole-pair field $M_{x\mu}$ as a complex auxiliary field describing the configuration of holon-pair accompanied with the RVB spinon pair at the sites x and $x+\mu$. So $M_{x\mu}$ should satisfy

$$\langle M_{x\mu}\rangle \sim \langle\bar\psi_{x+\mu}\big(z^\star_{x+\mu}z_x\big)\bar\psi_x\rangle. \tag{2.38}$$

This hole-pair field $M_{x\mu}$ is nothing but annihilation operator of spin-singlet electron pair sitting NN sites as mentioned. Explicitly, we use the Hubbard-Stratonovich transformation for $A_{\rm SC}$ as Eq.(2.28),

$$\begin{aligned}&\exp\left(\frac{J}{4}\Big|\bar\psi_{x+\mu}\big(z^\star_{x+\mu}z_x\big)\bar\psi_x\Big|^2\right)\\ &=\int dM_{x\mu}\exp\Big[-\frac{J\beta}{4}\bar M_{x\mu}M_{x\mu}\\ &\quad+\frac{J\beta}{4}\Big(M_{x\mu}\psi_x\big(\bar z^\star_{x+\mu}\bar z_x\big)\psi_{x+\mu}+\text{c.c.}\Big)\Big].\end{aligned} \tag{2.39}$$

This assures us of Eq.(2.38).

To study the effect of $A_{\rm SC}$, we start with Z of Eq.(2.10) and rewrite $A_{\rm SC}$ in the action by using Eq.(2.39). Then we integrate out the holon variables ψ_x as in the previous case (without $A_{\rm SC}$ there) to obtain the effective action, $A_{\rm full}$, where the suffix "full" implies $A_{\rm SC}$ is taken into account. The partition function of the full model is now given as

$$\begin{aligned}&Z_{\rm full}\equiv\int[dz][dU][dV][dM]\exp(A_{\rm full}),\\ &A_{\rm full}=A_{UV}+A_M=A_{\rm AF}+A_V+A_M.\end{aligned} \tag{2.40}$$

In addition to the action of the UV model of Eq.(2.36), $A_{\rm full}$ includes an extra term $A_{\rm M}(z_x, M_{x\mu})$ that depends on z_x and $M_{x\mu}$.

We have calculated A_M in the order up to $O((c_3)^4)$[7]. Eq.(2.39) shows that as ψ_x and $\psi_{x+\mu}$ hop, they leave the factor $M_{x\mu}\bar z^\star_{x+\mu}\bar z_x$, i.e., $M_{x\mu}$ is always accompanied with the AF component of spinon, (c.c. of) $z^\star_{x+\mu}z_x$. The hopping term $A_{\rm hop}$ itself supplies the FM component $\bar z_x z_{x+\nu}(\sim|\bar z_x z_{x+\nu}|V_{x\nu})$ along the link $(x,x+\nu)$ ψ_x hops. In expressing A_M we prefer to use $U_{x\mu}$ instead of $\bar z^\star_{x+\mu}\bar z_x$ using Eq.(2.17), because it makes the gauge invariance of the system manifest. Then $M_{x\mu}$ appears in A_M in the combination $M_{x\mu}(\bar z^\star_{x+\mu}\bar z_x)\sim M_{x\mu}|z^\star_{x+\mu}z_x|U_{x\mu}$. So we define a new variable,

$$M^\star_{x\mu}\equiv M_{x\mu}U_{x\mu}\sim\bar\psi_{x+\mu}\bar\psi_x. \tag{2.41}$$

and write A_M in terms of $M^\star_{x\mu}$ and $V_{x\mu}$, the latter is supplied by $A_{\rm hop}$. We note that $M^\star_{x\mu}$ is not gauge-invariant and represents the "holon pair" at $(x,x+\mu)$ in contrast with gauge-invariant $M_{x\mu}$ for "hole pair".

In the practical calculations in Sect.IV, we focus on the phase degrees of freedom of $M^\star_{x\mu}$, ignoring fluctuations of the radial part of $M^\star_{x\mu}$ as in the case of $W_{x\mu}\to V_{x\mu}$ (the London limit). So we set

$$\begin{aligned}&M^\star_{x\mu}=M\exp(i\varphi_{x\mu}),\\ &M\simeq\sqrt{\text{holon-pair density}}\sim\delta,\end{aligned} \tag{2.42}$$

and $dM_{x\mu}=d\varphi_{x\mu}/(2\pi)$. We include M into the coefficients of $A_{\rm M}$ and treat $M_{x\mu}=\exp(i\varphi_{x\mu})$ as a U(1) variable. Furthermore, we regard $|\bar z_x z_{x+\mu}|$ and $|z^\star_{x+\mu}z_x|$ involved in A_M as constants. They are also absorbed in the coefficients. The reason of this treatment is given below on the determination of the coefficients.

In terms of this $M^\star_{x\mu}$, A_M is expressed as

$$\begin{aligned}A_M=&\frac{f_1}{2}\sum_{x,\mu\neq\nu}M^\star_{x\mu}\bar M^\star_{x+\nu,\mu}V_{x+\mu,\nu}V_{x\nu}\\ &+\frac{f_2}{2}\sum_{x,\mu<\nu}\alpha_{\mu\nu}\Big[V_{x\nu}V_{x+\nu,\mu}\bar M^\star_{x+\mu,\nu}M^\star_{x\mu}\\ &\qquad+V_{x\nu}\bar M^\star_{x+\nu,\mu}M^\star_{x+\mu,\nu}\bar V_{x\mu}\\ &\qquad+M^\star_{x\nu}\bar M^\star_{x+\nu,\mu}V_{x+\mu,\nu}V_{x\mu}\\ &\qquad+\bar M^\star_{x\mu}\bar V_{x+\nu,\mu}V_{x+\mu,\nu}M^\star_{x\mu}\Big]\\ &+\frac{f_3}{2}\sum_{x,\mu<\nu}\bar M^\star_{x\nu}M^\star_{x+\nu,\mu}\bar M^\star_{x+\mu,\nu}M^\star_{x\mu}\\ &+\text{c.c.}.\end{aligned} \tag{2.43}$$

Each term in A_M is schematically shown in Fig.1. The terms with the coefficients f_1 and f_2 in Eq.(2.43) describe the local hopping of the holon-pair field $M^\star_{x\mu}$, whereas the f_3-term controls fluxes of $M^\star_{x\mu}$ penetrating each plaquette. These fluxes correspond to vortex excitations in the SC state. In other words, the f_1 and f_2-terms induce a primordial SC state and a genuine SC state is generated

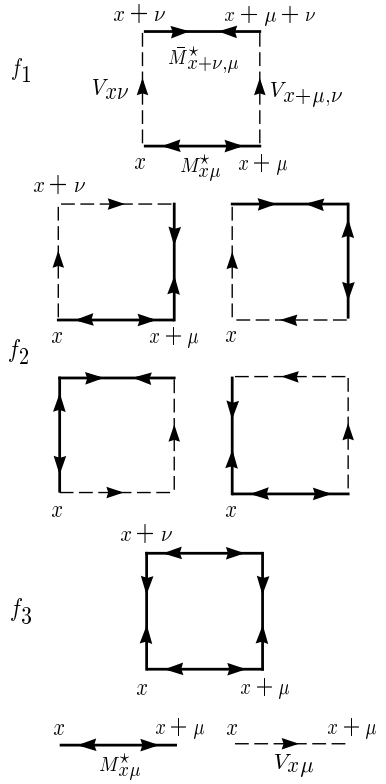

FIG. 1. Each term of $A_{\rm M}$ of Eq.(2.43). The lines with the reversed arrows indicate complex-conjugate variables, $\bar{M}^\star_{x\mu}$, $\bar{V}_{x\mu}$. The gauge invariance under Eq.(2.16) forces the arrows near each corner to make a divergenceless flow.

by the f_3-term. Numerical investigations in the following sections verify this qualitative expectation.

As stated in Sect.I, we think that a SC state is to be realized in a metallic phase, i.e., beyond the region of applicability of the leading order of the hopping expansion. So keeping the results of the hopping expansion for the three coefficients f_i of A_M is not suitable for discussing a SC state. For example, the coefficient f_3 is negative in the leading order of the hopping expansion, which favors the $s+id$-wave SC. We examined higher-order terms of the hopping expansion and found that some of them generate a positive value of f_3 to support the d-wave SC as observed experimentally. So in the following numerical studies, we shall assume that f_i's are positive and proportional to δ^2,

$$f_1, f_2, f_3 \propto \delta^2. \tag{2.44}$$

and treat their coefficients as *positive* free (phenomenological) parameters[18]. In short, all the effect of $|M_{x\mu}|$, $|\bar{z}_x z_{x+\mu}|$ and $|z^\star_{x+\mu} z_x|$ in and near the SC state are included in the effective coefficients f_i of A_M.

Also we have incorporated in Eq.(2.43) the layered-structure of the 3D lattice of cuprates[11] by introducing in Eq.(2.43) the anisotropy parameter $\alpha_{\mu\nu}$, which is defined as

$$\alpha_{\mu\nu} = \alpha_{\nu\mu} = \begin{cases} 1 & (\mu,\nu \neq 3) \\ 0 & (\mu \text{ or } \nu = 3) \end{cases} . \tag{2.45}$$

The layered structure of the system is systematically incorporated in the original Hamiltonian (2.1) by making the parameters t and J anisotropic. This induces anisotropies in the effective model that we have derived. Most of the terms are insensitive to the anisotropy except the f_2-term, which is the reason that we treat $A_{\rm hop}$ and A_V in a symmetric manner. For the f_2-term, the layered structure plays an important role to avoid frustrations and make the symmetry of SC to be $d_{\rm x^2-y^2}$.

III. PHASE STRUCTURE OF THE UV MODEL: AF AND MI TRANSITIONS

In this section, we study the UV model with the action $A_{UV} = A_{\rm AF} + A_V$ in Eq.(2.36) by means of the MC simulations. The full model $A_{\rm full} = A_{\rm AF} + A_V + A_M$ shall be studied in Sect.IV. For MC simulations, we consider a 3D cubic lattice of the size $V \equiv L^3$ (L up to 30) with the periodic boundary condition. We used the standard Metropolis algorithm for local update. Average number of sweeps was 2×10^5, and acceptance ratio was about $\sim 40\%$.

To study the phase structure of the model, we measured the internal energy E and the specific heat C, which are defined as

$$E = -\frac{1}{L^3}\langle A\rangle, \quad C = \frac{1}{L^3}\langle (A - \langle A\rangle)^2\rangle, \tag{3.1}$$

as functions of the parameters c_1, c_4 and c_5. We note that the c_4 term and c_5 term are related with each other because both are generated by c_3 term. Below we respect this correlation by setting the parameter c_5 as $c_5 \propto c_4$.

By obtaining the locations of the phase transition lines by the peaks of C, etc., we get a phase diagram in the $c_4 - c_1$ plane. Then we investigate spin correlation functions and instanton densities in order to identify the physical meaning and properties of each phase. To support this procedure, we also investigated fluctuations of each term of the action by measuring the individual "specific heat" C_{Ai} defined by

$$C_{A_i} \equiv \frac{1}{L^3}\langle (A_i - \langle A_i\rangle)^2\rangle, \quad i = 1,4,5,$$
$$A_1 \equiv A_{\rm AF},\ A_{4,5} \equiv c_{4,5}\text{−term in } A_V. \tag{3.2}$$

At $c_4 = 0$ (i.e., at $c_3 = 0$), the system is reduced to the AF Heisenberg model with the action $A_{\rm AF}$ alone, which has a phase transition from the paramagnetic (PM) spin-disordered phase to the AF spin-ordered phase at $c_1 \sim 2.8$. We study how the location of this AF phase transition changes and whether new phases appear as the c_4-term is turned on. It is naturally expected that the AF phase transition shifts to low-T region (large c_1 region) as the parameter c_4 is increased because the c_4 term favors FM NN spin coupling.

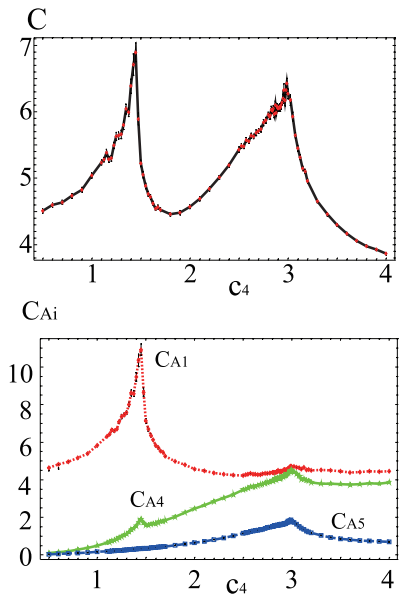

FIG. 2. Total specific heat C and specific heat of each term C_{A_i} of Eq.(3.2) as functions of c_4 for $c_1 = 3.5$ and $c_5 = c_4/3.0$. System size is $L = 30$. C has two peaks at $c_4 \simeq 1.5, 3.0$. C_{A_1} has a sharp peak at $c_4 \simeq 1.5$ suggesting the AF transition, and C_{A_4}, C_{A_5} have peaks at $c_4 \simeq 3.0$ suggesting the MI transition.

Let us first examine C and C_{A_i} as functions of c_4 for $c_1 = 3.5$. As we shall see later on, this value of c_1 belongs to relatively high-T region. In Fig.2 we show the result for the case $c_5 = c_4/3.0$. We found no anomalous behavior of E such as hysteresis, whereas C shown in Fig.2 exhibits two sharp peaks at $c_4 \simeq 1.5$ and 3.0. We verified that each peak has a systematic system-size (L) dependence, so we concluded that both peaks show existence of second-order phase transitions. C_{A_1} of Fig.2 exhibits a very sharp peak at $c_4 \simeq 1.5$. On the other hand, both C_{A_4} and C_{A_5} exhibit a peak at $c_4 \simeq 3.0$. Then we conclude that the AF phase transition takes place at $c_4 \simeq 1.5$ and the MI transition at $c_4 \simeq 3.0$.

The above conclusion may be confirmed by calculating the spin correlation function. In Fig.3, we show the correlation function $G_{\rm s}(r)$ of the O(3) spin $\vec{\ell}_x$ of Eq.(2.23),

$$G_{\rm s}(r) = \frac{1}{3L^3}\sum_{x,\mu}\langle \vec{\ell}_x \cdot \vec{\ell}_{x+r\mu}\rangle. \tag{3.3}$$

As we expected, at $c_4 = 0.7$, $G_{\rm s}(r)$ exhibits an oscillatory behavior and has a staggered magnetization,

$$\lim_{r\to\infty}(-)^r G_{\rm s}(r) \simeq (-)^{r_{\max}} G_{\rm s}(r_{\max}) \neq 0,$$
$$r_{\max} \equiv \frac{L}{2}, \quad \text{(AF phase)}. \tag{3.4}$$

So there exists an AF LRO at $c_4 = 0.7$. This confirms that the phase transition at $c_4 \simeq 1.5$ is the AF transition. At $c_4 = 2.2$ this AF order disappears and the system is

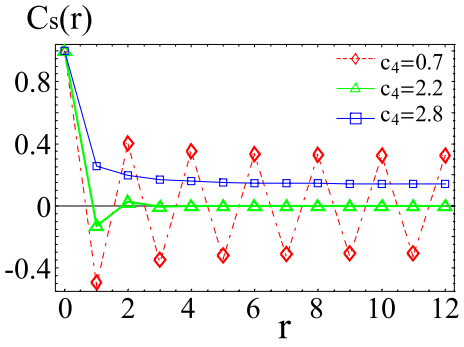

FIG. 3. Spin correlation function $G_s(r)$ of Eq.(3.3) for $c_1 = 3.5$, $c_5 = c_4/3.0$ and $L = 24$. At $c_4 = 0.7$, an AF LRO exists. At $c_4 = 2.2$, the AF LRO disappears. At $c_4 = 3.8$, a FM correlation appears as a result of existence of "free electrons".

in a magnetically disordered phase that we call paramagnetic (PM) phase. At $c_4 = 3.8$, $G_{\rm s}(r)$ exhibits a LRO,

$$G_{\rm s}(r_{\max}) \neq 0, \quad \text{(FM phase)}, \tag{3.5}$$

which implies that the system is in the FM phase. So we obtain a picture of the phase structure for $c_1 = 3.5$ that, as c_4 increases, the phase changes as AF $\to$ PM $\to$ FM.

We also calculated instanton densities of the gauge fields $U_{x\mu}$ and $V_{x\mu}$. For example, U-instanton density ρ_U is defined for $U_{x\mu} = e^{i\theta_{x\mu}}$, $\theta_{x\mu} \in [-\pi, \pi]$ in the following way[17, 19]. We first consider the magnetic flux $\Theta_{x\mu\nu}$ penetrating the plaquette $(x, x+\mu, x+\mu+\nu, x+\nu)$, which is defined as

$$\Theta_{x\mu\nu} \equiv \theta_{x\mu} + \theta_{x+\mu,\nu} - \theta_{x+\nu,\mu} - \theta_{x\nu},$$
$$(-4\pi \le \Theta_{x\mu\nu} \le 4\pi). \tag{3.6}$$

Then we decompose $\Theta_{x\mu\nu}$ into its integer part $n_{x\mu\nu}$, which represents the Dirac string (vortex line), and the remaining fractional part $\tilde{\Theta}_{x\mu\nu}$,

$$\Theta_{x\mu\nu} = 2\pi n_{x\mu\nu} + \tilde{\Theta}_{x\mu\nu}, \quad (-\pi \le \tilde{\Theta}_{x\mu\nu} \le \pi). \tag{3.7}$$

The U-instanton density $\rho_U(x)$ at the cube around the site $x + \frac{\hat{1}}{2} + \frac{\hat{2}}{2} + \frac{\hat{3}}{2}$ of the dual lattice is then defined as

$$\rho_U(x) = -\frac{1}{2}\sum_{\mu\nu\lambda}\epsilon_{\mu\nu\lambda}(n_{x+\mu,\nu\lambda} - n_{x,\nu\lambda})$$
$$= \frac{1}{4\pi}\sum_{\mu,\nu,\lambda}\epsilon_{\mu\nu\lambda}(\tilde{\Theta}_{x+\mu,\nu\lambda} - \tilde{\Theta}_{x,\nu\lambda}), \tag{3.8}$$

where $\epsilon_{\mu\nu\lambda}$ is the totally antisymmetric tensor. From the above definition, we define the average instanton density ρ_U as

$$\rho_U \equiv \frac{1}{L^3}\sum_x \langle|\rho_U(x)|\rangle. \tag{3.9}$$

The V-instanton density ρ_V is defined similarly for $V_{x\mu}$.

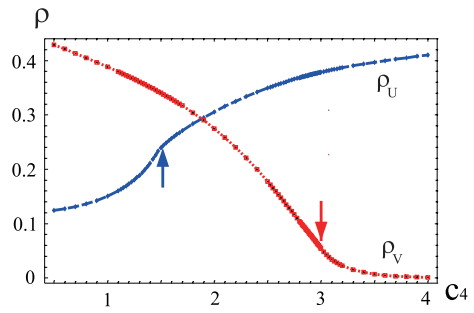

FIG. 4. Instanton densities ρ_U and ρ_V as functions of c_4 for $c_1 = 3.5$, $c_5 = c_4/3.0$ and $L = 30$. Arrows indicate the phase transition points determined by the specific heat (See Fig.2). At the first phase transition point $c_4 \simeq 1.5$, ρ_U starts to increase. On the other hand, at the second transition point $c_4 \simeq 3.0$, ρ_V tends to vanish.

The instanton density ρ_U measures strength of fluctuations of the gauge field $U_{x\mu}$. In the deconfinement phase of $U_{x\mu}$, fluctuations of $\Theta_{x\mu\nu}$ around its average $\Theta_{x\mu\nu} = 0$ are small and $\rho_U \simeq 0$. In the confinement phase of $U_{x\mu}$, on the other hand, $\Theta_{x\mu\nu}$ fluctuates violently, and ρ_U has a finite value. Here we note that the confinement by $U_{x\mu}$ field gives rise to quasi-excitations that are gauge-invariant "composite particles" in the AF channel. Such combinations include $z^{\star}_{x+\mu}U_{x\mu}z_x$, $\psi_{x+\mu}U_{x\mu}z_{x\sigma}$, etc. Similar interpretation holds for ρ_V concerning to the gauge dynamics of $V_{x\mu}$. The confinement here works in the FM channel, and the possible gauge-invariant quasi-excitations are $\bar{\psi}_x z_{x\sigma} = C_{x\sigma}$, $\bar{\psi}_x\psi_x$, $\bar{z}_{x\sigma}z_{x\sigma'}$ and their stretched versions such as $\bar{\psi}_{x+\mu}V_{x\mu}z_{x\sigma}$, etc.

In Fig.4 we show ρ_U and ρ_V for $c_1 = 3.5$. As we increases c_4, ρ_U starts to increase at the first phase transition at $c_4 \simeq 1.5$. This result means the fluctuation of $U_{x\mu}$ of AF NN spinon pairs become large, and the U-confinement spin-disordered phase appears. This result is consistent with the interpretation based on $G_s(r)$ above. On the other hand, at the second phase transition at $c_4 \simeq 3.0$, ρ_V tends to vanish. So, for $c_4 < 3.0$, the system stays in the V-confinement phase and holons and anti-spinons are bound within electrons as $\psi_x\bar{z}_{x\sigma}$. For $c_4 > 3.0$, the system is in the V-deconfinement phase, and holons and spinons start to hop coherently and independently as low-energy excitations. This indicates that the phenomenon of charge-spin separation[8] takes place and also the system is metallic.

Let us turn to the low-T region and see how the locations of these AF and MI phase transitions change. In Fig.5, we present the specific heat C and C_{A_i} for $c_1 = 6.5$. We again found two peaks at $c_4 \simeq 3.4$ and 5.4. Figs.5b, c show that both peaks develops systematically indicating that both phase transitions are of second order. Individual specific heat in Fig.5d shows that the peak of C at $c_4 \simeq 3.4$ corresponds to fluctuations of the c_4 and c_5-terms and so the MI transition, while the peak at $c_4 \simeq 5.4$

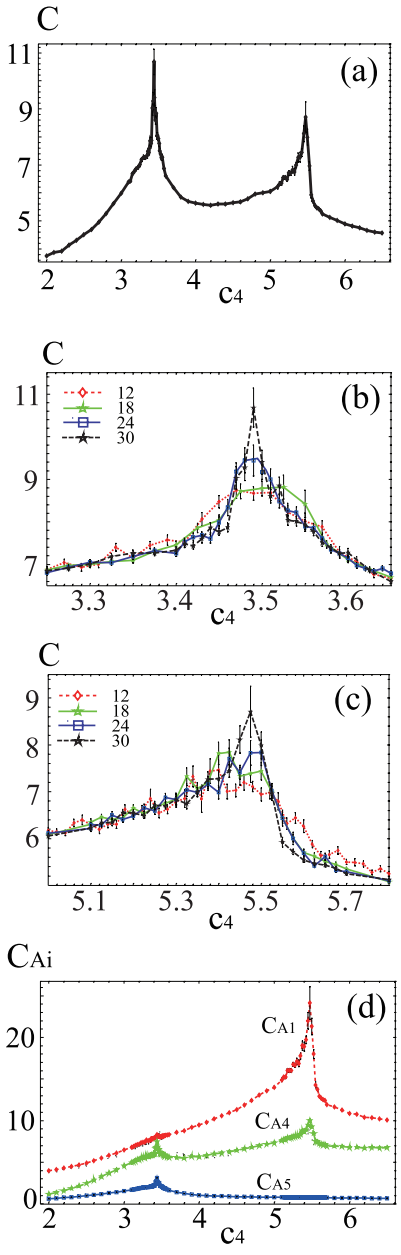

FIG. 5. Specific heat C as a function of c_4 for $c_1 = 6.5$ and $c_5 = c_4/3.0$. (a) C for $L = 30$. There are two peaks at $c_4 \simeq 3.4$, 5.4. (b,c) Each peak of C develops as the system size is increased. Results indicate that both phase transitions are of second order. (d) Specific heat C_{A_i} of each term. They indicate the transition at $c_4 \simeq 3.4$ is the MI one and the transition at $c_4 \simeq 5.4$ is the AF one.

is generated by the c_1-term and so the AF transition. Therefore the order of the AF and MI phase transitions along the c_4 axis has been interchanged compared to the previous high-T case of $c_1 = 3.5$.

To verify the above observation, we calculated the spin correlations, $G_s(r)$. The result is shown in Fig.6. In the intermediate region $3.4 < c_4 < 5.4$, $G_s(r)$ exhibits very

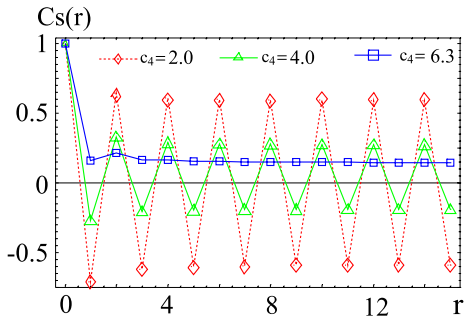

FIG. 6. Spin correlation function $G_s(r)$ for $c_1 = 6.5$, $c_5 = c_4/3.0$ and $L = 30$. At $c_4 = 2.0$, the oscillatory behavior around zero shows an AF order. At $c_4 = 4.0$, there is an AF order in the FM background order. At $c_4 = 6.3$, there is a FM order.

interesting behavior, i.e., an AF correlation exists in a FM background. This implies coexistence of the FM and AF orders. We note that a coexistence of FM and AM orders was also observed previously in the CP^1+Higgs boson model[20]. This model is a bosonic counterpart of the present model and the U(1) Higgs variable $\exp(i\alpha_x)$ there plays the role of the fermionic holon variable ψ_x.

In Fig.7 we present instanton densities. Compared with the high-T result of Fig.4, the result again indicates that two phase transitions have interchanged their order along the c_4 axis. As a result, there appears a range of c_4 in which both ρ_U and ρ_V are small, which implies that spinons and holons hop here both in U and V channels. In other words, charges are transported by holons whereas spin degrees of freedom are transported by spinons both in the AF and FM channels.

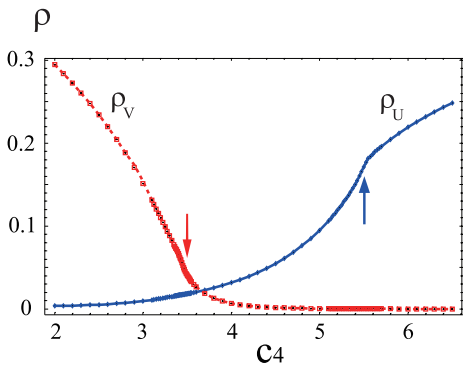

FIG. 7. Instanton densities ρ_U and ρ_V as functions of c_4 for $c_1 = 6.5$, $c_5 = c_4/3.0$ and $L = 30$. Arrows indicate the phase transition points determined by the specific heat (See Fig.5). At the first transition point $c_4 \simeq 3.4$, ρ_V tends to vanish. On the other hand, at the second transition $c_4 \simeq 5.4$, ρ_U gets large values showing that the system enters into the U-confinement phase.

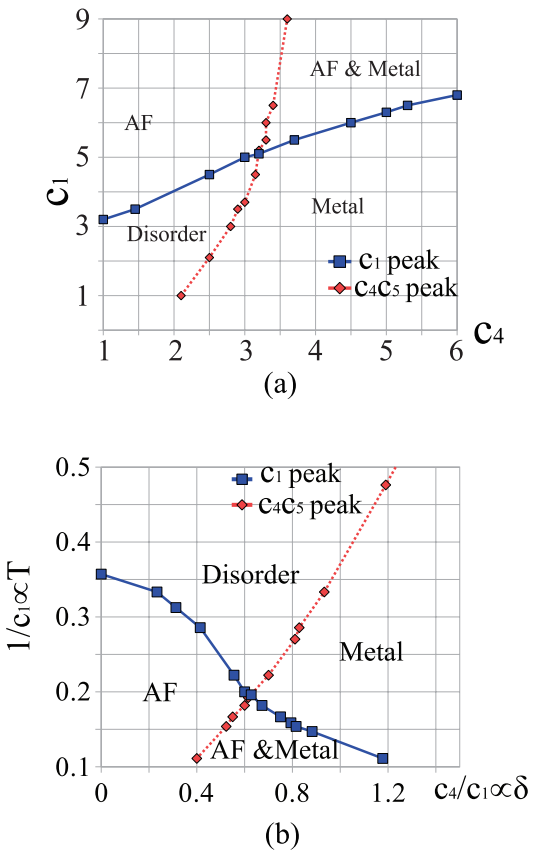

FIG. 8. Phase diagram of the UV model for $c_5 = c_4/3.0$. (a) in the c_4-c_1 plane, and (b) in the δ-T plane. Each phase is separated by two transition lines; the AF transition line and MI transition line. All the transitions are of second order.

We repeated similar calculations for various values of c_1 and c_4 and obtained the phase diagram of the model for $c_5 = c_4/3.0$. In Figs.8, we present the phase diagram; Fig.8a in the $c_4 - c_1$ plane and Fig.8b in the $\delta - T$ plane, the latter is obtained from the former by using Eq.(2.35).

So far, we have studied the case of $c_5/c_4 = 1/3.0$. We also studied other values of the ratio c_5/c_4 and found similar phase diagram to that in Figs.8. As the value of c_5/c_4 is increased, the MI transition line shifts to the region of smaller δ. This is expected from Eq.(2.33) because larger c_5/c_4 implies smaller critical value of c_4, and therefore smaller critical δ from Eq.(2.35).

To estimate roughly the critical δ of the MI transition, which we call $\delta_{\rm MI}$, for real materials, one may put $J \simeq 0.1$eV, $t \simeq 0.3$eV so $J/t \simeq 1/3$. Then we have $\delta \sim (J/t)^2 \cdot (c_4/c_1) \simeq 0.1(c_4/c_1)$ from Eq.(2.35). For $c_1 \sim 10.0$ ($T \sim 100$K), the critical line of Fig.8a shows $c_4/c_1 \sim 0.4$, and this formula gives rise to $\delta_{\rm MI} \simeq 0.04$. As discussed below Eq.(2.33) the higher-order terms in Eq.(2.28) enhance the metallic phase, so the MI phase transition line is expected to be located in very underdoped region $\delta \ll 1$.

IV. PHASE STRUCTURE OF THE FULL MODEL: SC TRANSITION

In this section, we study the full model of Eq.(2.40) with the action $A_{\rm full} = A_{\rm AF} + A_{\rm V} + A_{\rm M}$. Besides the AF and MI transitions observed in the previous section, we expect that the new term $A_{\rm M}$ in the action generates condensation of the hole-pair field $M_{x\mu}$ and/or the holon-pair field $M^{\star}_{x\mu}$ as the hole density δ is increased. This condensation implies generation of a SC state.

We studied the system $A_{\rm full}$ by means of the MC simulations. As $M^{\star}_{x\mu}$ is a composite of holons at x and $x+\mu$, we put $f_{1,2,3} \propto \delta^2 \propto c_4^2$ and $M^{\star}_{x\mu} \in U(1)$ as explained in Sect.II. Physically, the proportional constants f_i/c_4^2 $(i = 1, 2, 3)$ depend on the density of holes that actually participate in the SC fluid. We studied the system $A_{\rm full}$ for various values of f_i/c_4^2 and found that the system is stable only for the case with small values of f_i/c_4^2. For example, the AF phase disappears at very small value of c_4 for $f_i/c_4^2 \sim O(1)$. In this section, we explicitly show the results for the case with $f_1 = f_2 = f_3 = 0.03\, c_4^2$.

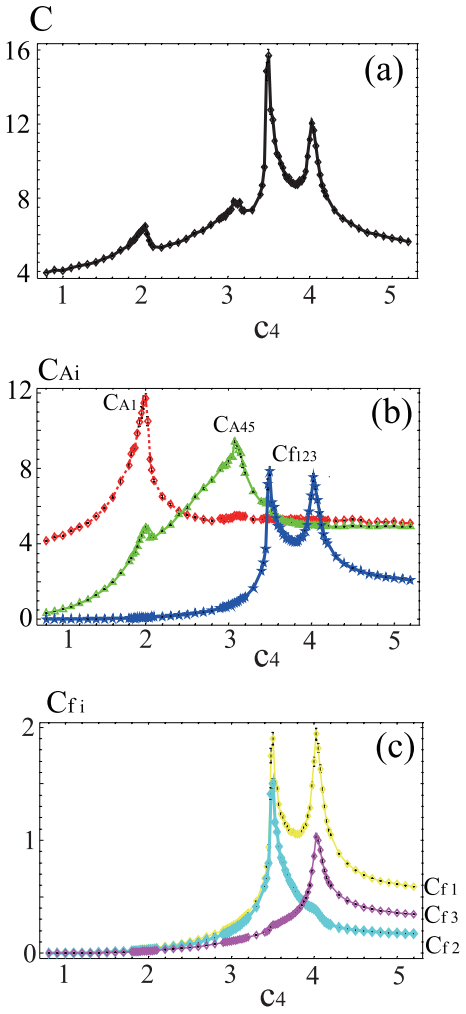

FIG. 9. Specific heat (a) C, (b) C_{A_i}, (c) C_{f_i} as functions of c_4 for $c_1 = 4.0$, $c_5 = c_4/3.0$ and $L = 24$. $C_{A_{45}}$ implies the fluctuatiuon of $A_4 + A_5$, and C_{f123} for $A_M = A_{f_1} + A_{f_2} + A_{f_3}$.

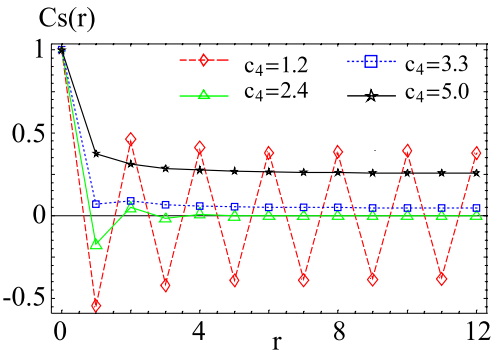

FIG. 10. Spin correlation functions for various values of c_4 for $c_1 = 4.0$, $c_5 = c_4/3.0$. $L = 24$. At $c_4 = 1.2$ there is an AF order; At $c_4 = 2.4$, no magnetic order; At $c_4 = 3.3$, a tiny FM order; At $c_4 = 5.0$, a FM order.

Let us first study the high-T region first by choosing $c_1 = 4.0$, $c_5 = c_4/3.0$. In Figs.9, we present various specific heat as functions of c_4. The total specific heat C in Fig.9a exhibits four peaks at $c_4 \simeq 2.0,\ 3.2,\ 3.5$ and 4.1. In order to identify the physical meaning of each peak, we show the individual specific heat C_{A_i} in Fig.9b and C_{f_i} $(i = 1, 2, 3)$ for the f_i-term in A_M defined similarly to Eq.(3.2) in Fig.9c. From these results, it is expected that the first two peaks correspond to the AF transition at $c_4 \simeq 2.0$ and the MI transition at $c_4 \simeq 3.2$. The remaining two terms correspond to fluctuations of f-terms in the action, and therefore the SC phase transition. More precisely, the third peak at $c_4 \simeq 3.5$ in C corresponds to the $f_1,\ f_2$-terms and the fourth one at $c_4 \simeq 4.1$ to the $f_1,\ f_3$-terms. We shall comment on them later.

In Fig.10 we present the spin correlation function $G_s(r)$ for various values of c_4. It is obvious that only at $c_4 = 1.2$ the AF LRO exists. At $c_4 = 5.0$, there is a solid FM order. This is consistent with the interpretation of four peaks above.

In order to study the symmetry of SC state, we consider the quantity M_2, the expectation value of $M_{x\mu}\bar{M}_{x+\mu,\nu}$ $(\mu \neq \nu)$, defined as

$$M_2 \equiv \frac{1}{8}\big\langle M_{x+1,2}\bar{M}_{x1} + \bar{M}_{x+2,1}M_{x+1,2} + \bar{M}_{x2}M_{x+2,1} + \bar{M}_{x2}M_{x1}\big\rangle + \text{c.c.} \qquad (4.1)$$

In Fig.11 we present M_2. It takes negative values and starts to develop significantly at $c_1 \sim 3.5$, i.e., at the third peak of C. It is obvious that a d-wave correlation between adjacent hole-pair fields is generated beyond the third peak.

We also measured the instanton densities ρ_U, ρ_V and $\rho_{M^\star}$. $\rho_{M^\star}$ is defined in a similar manner to ρ_U but by using the holon-pair field $M^{\star}_{x\mu} (\equiv M_{x\mu}U_{x\mu} \sim \bar{\psi}_{x+\mu}\bar{\psi}_x)$

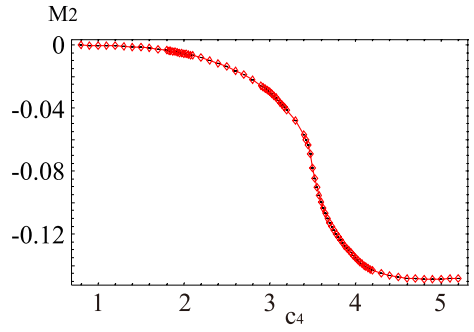

FIG. 11. Expectation value M_2 of Eq.(4.1) for $c_1 = 4.0$, $c_5 = c_4/3.0$, $L = 24$. The result shows that d-wave correlation between adjacent hole-pair fields starts to appear at $c_4 \sim 3.5$.

instead of $U_{x\mu}$. $\rho_{M^\star}$ reflects the vortex density of $M^\star_{x\mu}$. These three instanton densities are shown in Fig.12. By comparing Fig.12 with Fig.4 we see that the behavior of ρ_U and ρ_V is not influenced strongly by the existence of the f-terms, i.e., ρ_U starts to increase at $c_4 \simeq 2.0$ and ρ_V vanishes at $c_4 \simeq 3.2$. The $M^\star$-instanton density $\rho_{M^\star}$ rapidly starts to decrease at $c_4 \simeq 3.5$ and vanishes at $c_4 \simeq 4.1$. We think that the SC phase transition, which is signaled by vanishingly small $\rho_{M^\star}$, takes place at $c_4 \simeq 4.1$.

From the above numerical calculations, we understand the physical meanings of the two peaks at $c_4 \simeq 3.5,\ 4.1$ as follows. The third peak at $c_4 \simeq 3.5$ are generated by the f_1 and f_2-terms and is located just after the MI transition at $c_4 \simeq 3.2$. After the MI transition, the holon-hopping amplitude $V_{x\mu}$ becomes stable, and as a result, these f_1 and f_2 terms start to correlate the phases of *a pair of adjacent link fields* $M^\star_{x\mu}$. In fact, these two terms in Eq.(2.43) need a stabilized $V_{x\mu}$ to let $M^\star_{x\mu}$ stabilize. Fig.12 shows that $\rho_{M^\star}$ at $c_4 \simeq 3.5$ is still large. So this effect is not strong enough to stabilize the holon-pair field

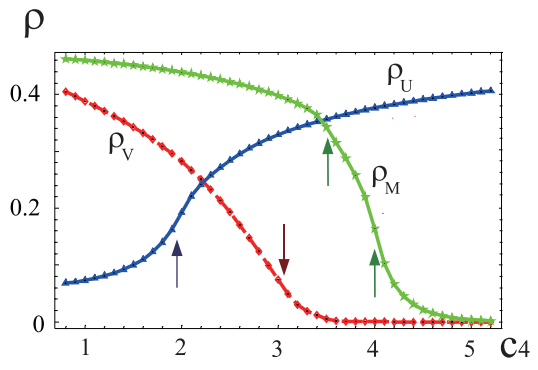

FIG. 12. Instanton densities ρ_U, ρ_V and $\rho_{M^\star}$ as a function of c_4 for $c_1 = 4.0$, $c_5 = c_4/3.0$ and $L = 12$. Arrows indicate the locations of four peaks in C of Fig.9.

$M^\star_{x\mu}$ completely at this region of c_4. In order to suppress vortex excitations of the holon-pair field $M^\star_{x\mu}$ (making $\rho_{M^\star}$ small enough), sufficient amount of the f_3-term is necessary. The fourth peak of C at $c_4 \simeq 4.1$ corresponds to the critical value of f_3 to realize such $M^\star_{x\mu}$ stabilization with phase coherence and generation of SC. These consideration leads to our conclusion that the genuine SC starts at the fourth peak $c_4 \simeq 4.1$.

From the above consideration, we expect that the region between the third and fourth peaks corresponds to a primordial SC state. In this region we expect that holons acquire a pseudo-gap. In fact, as $M^\star_{x\mu}$ couples to ψ_x as $M^\star_{x\mu}\psi_{x+\mu}\psi_x$, finite expectation value of $M^\star_{x\mu}$ supplies fermion-number nonconserving hopping processes effectively. Together with the fermion-number preserving hopping term supplied in $A_{\rm hop}$ these processes give rise to a gap in excitation energy of holons[21].

Furthermore, from the local gauge symmetry of the system, the terms like $\bar{M}^\star_{x\mu}z_{x+\mu}z_x$ are also to be generated by the renormalization effect of high-energy modes

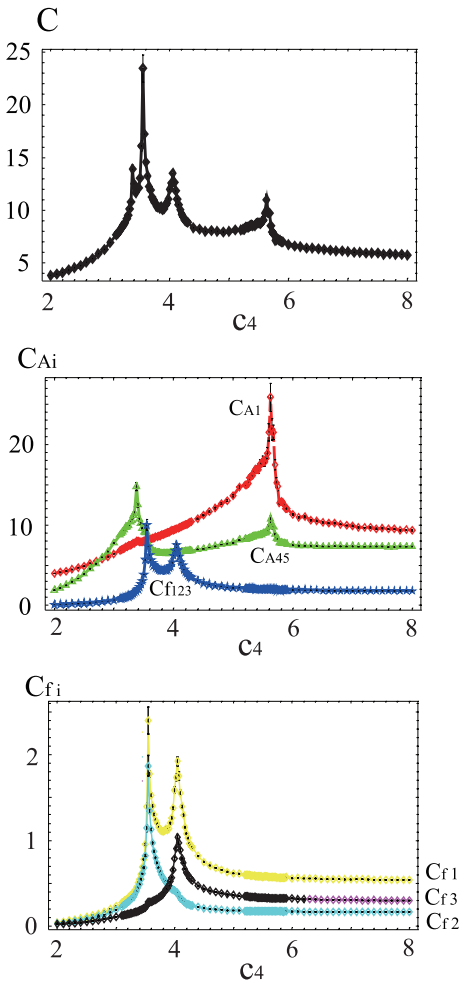

FIG. 13. Specific heat C, C_{A_i} and C_{f_i} as functions of c_4 for $c_1 = 6.5$, $c_5 = c_4/3.0$ and $L = 24$.

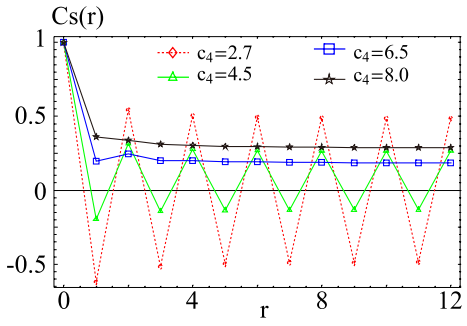

FIG. 14. Spin correlation functions $G_s(r)$ for various values of c_4 with $c_1 = 6.5, c_5 = c_4/3.0$. At $c_4 = 2.7$ there is an AF order; at $c_4 = 4.5$, an AF order in a FM background; at $c_4 = 6.5$, and $c_4 = 8.0$, a FM order.

of z_x and ψ_x. Then the spinon field z_x also acquires an extra contribution to its pseudo-gap, irrespective of a possible pseudo-gap expected by the mixing of two channels, $c_1 U_{x\mu} z^\star_{x+\mu} z_x$ and $c_4 V_{x\mu} \bar{z}_{x+\mu} z_x$. Anyway, the physical properties of that state such as excitation spectrum is interesting and should be reserved as a future problem.

Next, let us study the system $A_{\rm full}$ at lower-T region by setting $c_1 = 6.5$, $c_5 = c_4/3.0$. Behavior of various specific heats, C, C_{A_i}, C_{f_i} are shown in Fig.13. There are again four peaks in the total specific heat C at $c_4 \simeq 3.4$, 3.6, 4.0 and 5.6. From the behavior of C_{A_i} and C_{f_i} the first peak at $c_4 \simeq 3.4$ corresponds to the MI transition, the peak(s) at $c_4 \simeq 4.0$(and 3.6) to the SC transition, and the fourth peak at $c_4 \simeq 5.6$ to the AF transition. The order of these transitions is different from that at the previous high-T case as we have already seen in the UV model. In order to verify the above identification, we calculated the spin correlation functions $G_s(r)$, the expectation value of adjacent hole-pair field M_2, and the instanton densities as before. We show the results in Figs.14, 15 and 16.

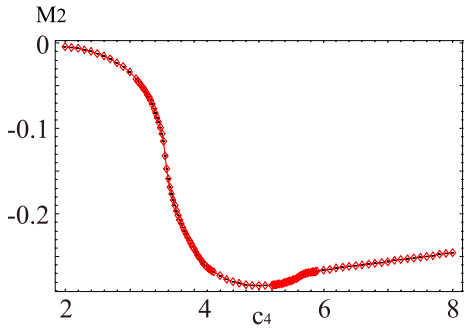

FIG. 15. Expectation value M_2 for $c_1 = 6.5$, $c_5 = c_4/3.0$, and $L = 24$. The result shows that d-wave correlation between adjacent hole-pair fields appears at $c_4 \sim 3.6$. It is interesting to observe that the correlation decreases slightly in the region *without* the AF LRO $c_4 > 5.6$.

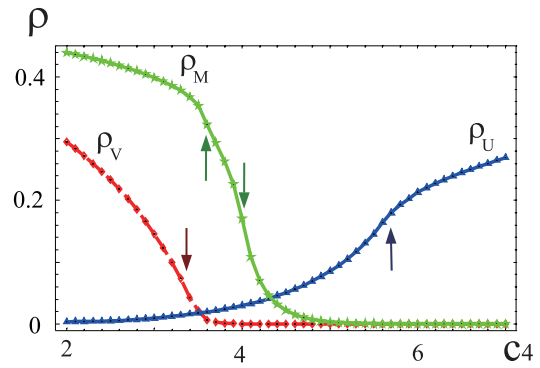

FIG. 16. Instanton densities ρ_U, ρ_V and $\rho_{M^\star}$ as functions of c_4 for $c_1 = 6.5$, $c_5 = c_4/3.0$ and $L = 12$. Arrows indicate the phase transition points determined by the specific heat (See Fig.9). Their behavior is consistent with the phase transition discussed in the text based on Fig.9.

These results support the interpretation of each phase given above.

In Fig.17, we present the obtained phase diagram of the full model $Z_{\rm full}$ of Eq.(2.40) in the $\delta - T$ plane. Each phase are separated by three transition lines for AF, MI, and SC transitions. The SC phase always exists inside the metallic phase, whereas there is the coexisting phase of the AF and SC at the low-T region. In addition to these three lines, one may add the line corresponding to the primordial SC transition as the line of pseudo-gap generation. Except for the pseudo-gap transition, which seems not to be a sharp transition in experiments, this

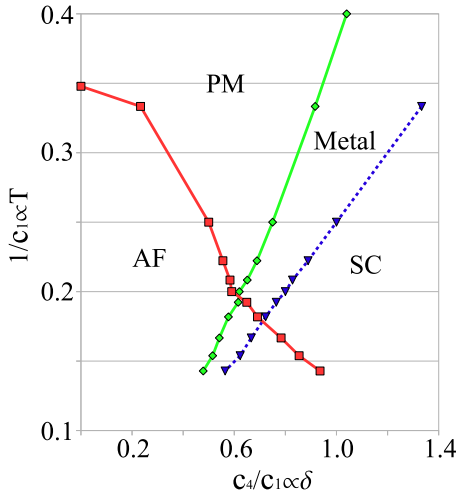

FIG. 17. Phase diagram of the full model of Eq.(2.40) in the δ-T plane. The three lines for AF transition, MI transition and SC transition separate each phase. All the transitions are of second order. One may add the pseudo-gap transition line as the fourth line.

phase diagram is consistent with that observed experimentally for homogeneous clean underdoped samples[10].

V. CONCLUSION AND DISCUSSION

In the present paper, we have studied the phase structure in the underdoped region of the t-J model by using the slave-fermion representation. In this formalism, the AF-insulator phase naturally appears and it is expected that beyond a critical hole concentration $\delta_{\rm MI}$ the coherent hopping of holes is generated and the system enters into the metallic phase. This phenomenon was previously studied by the mean-field theory, and the critical hole concentration was estimated as $\delta_{\rm MI} = 0$[22].

We investigated the system by integrating out the fermionic holon field by the hopping expansion, which is legitimated for the region in and near the insulating phase, and then numerically studied the AF, MI and SC phase transitions. The obtained phase diagram is consistent with that observed experimentally for clean and homogeneous samples at small hole concentrations. The present study also implies that the observed pseudo-gap corresponds to a primordial formation of SC order parameter $M_{x\mu}$.

For the SC phase transition, we have treated the coefficients of effective action in more flexible manner than the original hopping expansion although we maintain the structure of interaction terms. As explained, this is because these coefficients certainly acquire renormalization and even change their signature as we go into the SC state. Some of our results in the present paper may reflect this flexibility, i.e., they may not be possible in the original t-J model due to the restrictions among the coefficients. The pseudo-gap transition might disappear (merge to the genuine SC transition) with different treatments of the coefficients. Even in such case, the results obtained in the present paper have important meaning as the knowledge of a reference system to the t-J model and other canonical models of the high-T_c materials.

Concerning to the SC order parameter, we proposed gauge-invariant $M_{x\mu}$ for hole pairs as a most direct possibility[7]. We have calculated its correlation function $\langle \bar{M}_{x\mu} M_{y\nu} \rangle$, but found no LRO of $M_{x\mu}$ even in the SC phase. We understand this in the following way. If one could calculate this correlation of the t-J model exactly, one would have LRO in the SC state. The effective model in exact treatment certainly contains a lot of nonlocal interaction terms among $M_{x\mu}$, although their coefficients are small. Nonvanishing LRO is to be supported by these nonlocal interactions. However, the present model truncates the effective interaction terms to short-range ones, and so fails to produce LRO of $M_{x\mu}$.

However, the study of lattice gauge theory[23] provides us with a viable alternative of describing a SC state. An effective system may involve only short-range interactions but it may generates the Higgs phase in which Meissner effects takes place actually. The price to pay is that there are no local order parameters to signal LRO. Our present model with the action A_M is just a such model. Because our gauge-noninvariant $M^\star_{x\mu}$ for holon pairs has vanishing correlations due to gauge-invariant action due to Elitzur's theorem[24], one need to introduce complicated nonlocal order parameters[25] to show that some kind of LRO exists. Here we note that existence of LRO is a beautiful theoretical criteria to demonstrate SC phenomenon, but not a necessary condition. A simple and direct proof of a SC state may be to measure the mass of external electromagnetic field and demonstrate the Meissner effect, i.e., the Higgs mechanism. We have not made such a proof, but the existence of anomalous peak of the specific heat certainly demonstrates a new phase, which should corresponds to the Higgs phase. In fact, we have considered a U(1) Ginzburg-Landau model[26], which is obtained from A_M of Eq.(2.43) by putting $V_{x\mu}$ to a certain constant. So the model loses gauge symmetry or viewed as a gauge-fixed version. The MC simulation of this model certainly exhibits a Higgs phase for sufficiently large f_i in which the correlation functions $\langle \bar{M}^\star_{x\mu} M^\star_{y\nu} \rangle$ exhibit a LRO. Let us summarize the situation. Because the faithful effective model of $M_{x\mu}$ is full of nonlocal interactions, we replace it by a short-range model. By sacrificing the LRO of gauge-invariant *local* order parameter, we are able to obtain the new phase. The analysis of the related model and the experience of lattice gauge theory strongly indicate this phase is a Higgs phase which is necessary to support SC.

The reason why we integrate out the fermionic holon field analytically is obvious, i.e. it is technically difficult to study fermion systems by numerical methods. In recent years, however, it has become possible to numerically simulate relativistic fermion systems and therefore it is important and also interesting to study the MI phase transition in the present system by means of those simulation methods. This problem is under study and we hope that the result will be reported in a future publication. Even in such a situation, the content of the present paper may be useful as some basis and a reference to obtain further understanding of physics of high-T_c superconductors.

Acknowledgment

This work was partially supported by Grant-in-Aid for Scientific Research from Japan Society for the Promotion of Science under Grant No.20540264.

Appendix A: Holon-field integration

In this appendix, we show some details of holon-field integration to derive Eq.(2.26). The same techniques are applicable to derive $A_{\rm M}$ in Eq.(2.43). It is useful to start with the original path-integral expression[7] in which Grassmann number $\psi_x(\tau)$ is a function of the

imaginary-time τ. This is because the ordering of variables is crucial to obtain the correct results. Then the relevant integration reads as

$$\begin{aligned}
&\int d\psi_x d\psi_{x+\mu} \exp\Big[\frac{c_3}{2\beta}\int_0^\beta d\tau\ (\bar{z}_{x+\mu}z_x)\bar{\psi}_x\psi_{x+\mu}(\tau) + \text{c.c.}\Big] \\
&= \Big(\frac{c_3}{2\beta}\Big)^2 |\bar{z}_{x+\mu}z_x|^2 \\
&\times \int_0^\beta d\tau_1 d\tau_2 \langle \bar{\psi}_{x+\mu}(\tau_1)\psi_x(\tau_1)\bar{\psi}_x(\tau_2)\psi_{x+\mu}(\tau_2)\rangle \\
&= -\Big(\frac{c_3}{2\beta}\Big)^2 |\bar{z}_{x+\mu}z_x|^2 \int_0^\beta d\tau_1 d\tau_2 \langle \psi_{x+\mu}(\tau_2)\bar{\psi}_{x+\mu}(\tau_1)\rangle \\
&\times \langle \psi_x(\tau_1)\bar{\psi}_x(\tau_2)\rangle \\
&= \delta\Big(\frac{c_3}{2}\Big)^2 |\bar{z}_{x+\mu}z_x|^2, \qquad \text{(A.1)}
\end{aligned}$$

where we have used the following Green function of the hopping expansion,

$$\begin{aligned}
&\langle \psi_x(\tau_1)\bar{\psi}_x(\tau_2)\rangle \\
&= \frac{e^{-m(\tau_1-\tau_2)}}{1+e^{-\beta m}}[\theta(\tau_1-\tau_2) - e^{-\beta m}\theta(\tau_2-\tau_1)]. \qquad \text{(A.2)}
\end{aligned}$$

In Eq.(A.2), m is the chemical potential and there holds the relation,

$$\delta = \langle \bar{\psi}_x(\tau+0)\psi_x(\tau)\rangle = \frac{e^{-\beta m}}{1+e^{-\beta m}}. \qquad \text{(A.3)}$$

[1] J. G. Bednorz and K. A. Müller, Z. Phys. **B64**, 189 (1986).

[2] See, e.g., N. Doiron-Leyraud, C. Proust, D. LeBoeuf, J. Levallois, J.-B. Bonnemaison, R. Liang, D.A. Bonn, W.N. Hardy, and L. Taillefer, Nature **447**, 565 (2007); D.A. Bonn, Nature Physics **2**, 159(2006).

[3] For reviews of theoretical approaches, see, e.g., P. W. Anderson, "The Theory of Superconductivity in the High-Tc Cuprate Superconductors" Princeton University Press (1997); P. A. Lee, N. Nagaosa, and X-G Wen, Rev. Mod. Phys. **78**, 17 (2006).

[4] P. W. Anderson, Science **235**,1196(1987).

[5] G. Kotliar and A. Ruckenstein, Phys.Rev.Lett.**57**,2790(1987), and references cited therein.

[6] D. Yoshioka, J. Phys. Soc. Japan **58**, 32 (1989).

[7] I. Ichinose and T. Matsui, Phys. Rev.**B45**, 9976 (1992).

[8] P. W. Anderson, Phys. Rev. Lett. **64**, 1839 (1990); I. Ichinose and T. Matsui, Nucl. Phys. **B394**, 281 (1993); N. Nagaosa, Phys. Rev. Lett. **71**, 4120 (1993;) I. Ichinose and T. Matsui, Phys. Rev. **B 51**, 11860 (1995); I. Ichinose, T. Matsui, and M. Onoda, Phys. Rev. **B 64**, 104516 (2001).

[9] G. Kotliar, Phys. Rev. **B37**, 3664 (1988); Y. Suzumura,Y. Hasegawa and H. Fukuyama, J. Phys. Soc. Japan **57**, 2768 (1988).

[10] H. Mukuda, M. Abe, Y. Araki, Y. Kitaoka, K. Tokiwa, T. Watanabe, A. Iyo, H. Kito, and Y. Tanaka, Phys. Rev. Lett. **96**, 087001 (2006).

[11] The cuprates have a layered structure of 2D copper-oxide planes in the xy plane stacked along the z axis. Reflecting it, the t-J model should have anisotropy in the coupling constants J and t of the Hamiltonian (2.1) for the xy directions and z direction, i.e., $J_z < J_{xy}$, $t_z < t_{xy}$. For explicit set up of asymmetry in the t-J model and calculation of the Neel temperature of the doped Heisenberg model, see H. Yamamoto, G. Tatara, I. Ichinose, and T. Matsui, Phys. Rev. **B44**, 7654 (1991). In this paper we write down the formula for the symmetric case for simplicity except for the hole-pair action A_M in Eq.(2.43), but extension to the anisotropic case is straightforward.

[12] The variable $z_x^\star$ should not be confused with $\bar{z}_x$ or z_x^*, the complex conjugate of z_x. In Ref.[7], the time-reversed spinon field $\tilde{z}_x \equiv i\sigma_2\bar{z}_x^{\rm t}$, $\tilde{z}_{x1} = \bar{z}_{x2}$, $\tilde{z}_{x2} = -\bar{z}_{x1}$ has been introduced. $z_x^\star$ here is just its complex conjugate, i.e., $z_{x\sigma}^\star = \bar{\tilde{z}}_{x\sigma}$. In this paper a bar-symbol implies the complex conjugate for a complex number and the Grassmann conjugate for a Grassmann number. We do not use asterisks in this paper.

[13] We use the coefficient c_3 instead of c_2. This is partly because c_2 has been reserved for the coefficient of plaquette term $\bar{U}_{x\nu}\bar{U}_{x+\nu,\mu}U_{x+\mu,\nu}U_{x\mu}$, a possible interaction term that may be included in the generalization of the model. In this viewpoint, we set $c_2 = 0$ in this paper.

[14] Their explicit form and roles are discussed in details in Ref.[7].

[15] F. A. Berezin, "The Method of Second Quantization" (Academic, New York, 1966); Y. Ohnuki and T. Kahsiwa, Prog. Theor. Phys. **60**, 548 (1978).

[16] We should remark that the signatures in front of λ_x and $\lambda_{x+\mu}$ in the exponent of $U_{x\mu}$ are the same and not the opposite. This is in contrast with the usual lattice gauge theory.

[17] S. Takashima, I. Ichinose, and T. Matsui, Phys. Rev. **B72**, 075112 (2005).

[18] Strictly speaking, $f_3 \propto \delta^4$ in the leading order. Here we take the simpler assumption for simplicity of the numerical study.

[19] T. A. DeGrand and D. Toussaint, Phys. Rev.**D22**, 2478 (1980).

[20] K. Aoki, K. Sakakibara, I. Ichinose, T. Matsui, Phys. Rev. **B80**, 144510 (2009); Y. Nakano, T. Ishima, N. Kobayashi, K. Sakakibara, I. Ichinose, T. Matsui, e-Print arXiv:1005.3997.

[21] The mechanism discussed here to generate a gap is a standard one through a mixing of normal channel and SC channel. A typical example is the Bogoliubov transformation in the Bardeen-Cooper-Schriefer model of conventional superconductivity. For bosonic spinon excitations, one needs a bosonic version of Bogoliubov transformation.

[22] B. I. Shraiman, E. D. Siggia, Phys. Rev. Lett. **61**, 467 (1988); Z. B. Su, Y. M. Li, W. Y. Lai, and L. Yu, Phys.

Rev. Lett. **63**, 1318 (1989).
[23] J. Kogut, Rev. Mod. Phys. **51**, 655 (1979).
[24] S. Elitzur, Phys. Rev. **D12**, 3978 (1975).
[25] For the model including matter fields, Wilson loop[23] exhibits perimeter law even in the confinement phase, so it cannot be used as a nonlocal order parameter. For nonlocal order parameters in such a case, see, e.g., K. Fredenhagen and M. Marcu, Commun Math. Phys. **92**, 81 (1983); J. Bricmont and J. Froehlich. Phys. Lett. **B122**, 73 (1983).
[26] T. Shimizu, S. Doi, I. Ichinose, T. Matsui, Phys. Rev. **B79**, 092508 (2009). See also T. Ono, Y. Moribe, S. Takashima, I. Ichinose, T. Matsui, and K. Sakakibara, Nucl. Phys. **B764**, 168 (2007).